Submitted to:
2001 Particle Accelerator Conference;
June 18-22, 2001; Chicago, IL

BNL-67937

FITTING HELICAL SNAKE AND ROTATOR FIELD STRENGTH MEASUREMENTS IN RHIC

V. Ranjbar, A. U. Luccio,W. W. MacKay, N. Tsoupas, BNL, Upton, NY

Abstract

We examined recent multi-pole measurements for the helical snakes and rotators in RHIC to generate a full field map. Since multi-pole measurements yield real field values for B_ρ field components we developed a unique technique to evaluate the full fields using a traditional finite element analysis software [1]. From these measurements we employed SNIG [2] to generate orbit and Spin plots. From orbit values we generated a transfer matrix for the first snake.

1 FIELD ANALYSIS PROBLEM

Much work has been done on predicting the field structure of the newly installed helical snakes and rotators in RHIC. Analytical[3] [4] [5] [7] and Numerical [6] work has been conducted to generate an appropriate model for these elements. But up to now actual field measurements taken from the real magnets have not been analyzed. A comparison of the actual field values with current analytical models proved problematic in terms of fitting. In addition to the problem of modeling the end effects and accounting for the quadrupole fields, we found a general longitudinal dependence for the multi-poles in the helical basis. Since this longitudinal dependence could not be accounted for in a neat analytical solution and required resorting to a series solution expansion we decided that using an available finite element analysis program would be a more efficient method to generate a solution.

However current finite element analysis programs are designed to solve Laplace's equation for cases with a scalar potential boundary condition. Since we possessed multi-pole data appropriate for the generation B_ρ field components along a 3.1 cm radius, we needed to develop a magnetic scalar potential along a cylindrical surface to use the software to solve the interior field problem. Considering that the B_ρ component must satisfy Laplace's equation separately:

$$\nabla^2 B_\rho = 0 \tag{1}$$

We can use TOSCA [1] to solve this version of Laplace's equation thus giving B_ρ everywhere interior to our boundary conditions ($\rho_0 = 3.1$ cm). Using this B_ρ we can evaluate the real magnetic scalar potential Φ_M using:

$$\Phi(\rho_0)_M = \int_0^{\rho_0} B_\rho d\rho + \Phi(0)_M \tag{2}$$

Finally using our derived values for Φ_M we can again use TOSCA [1] as it was intended, generating a useable full field model contained in the OPERA-TOSCA [1] operating environment.

Since we are equipped to solve for fields internal to our known boundary conditions, we are restricted to considering transverse particle motion of $\rho < 3.1$ cm. Given a beam pipe with an internal radius of 4.5 cm it would be better if we could account for displacements up to at least 4.1 cm. To accomplish this we simply linearly extrapolated the straight magnetic field formula for B_ρ

$$B_\rho = B_0 \sum_{n=0}^{\infty} \left(\frac{\rho}{\rho_0}\right)^n [a_n \cos((n+1)\theta) + b_n \sin((n+1)\theta)] \tag{3}$$

by simply using existing multi-pole values and evaluating B_ρ at a 4.1cm radius.

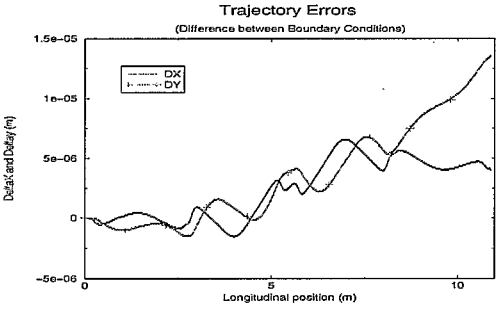

Figure 1: Difference in x and y trajectories for Fields evaluated with boundary conditions at 3.1 cm and 4.1 c.m.

From Fig 1 it seems clear that using a 4.1 cm radius for the boundary conditions will give reasonable orbit results.

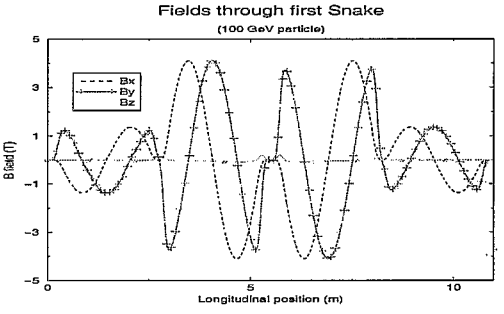

Figure 2: B_x ,B_y and B_z fields evaluated along 100 GeV particle path.

2 ORBITAL TRAJECTORY THROUGH FIRST SNAKE

Using SNIG [2] we track 100 GeV proton through the Field map of a single snake. Results were consistent with

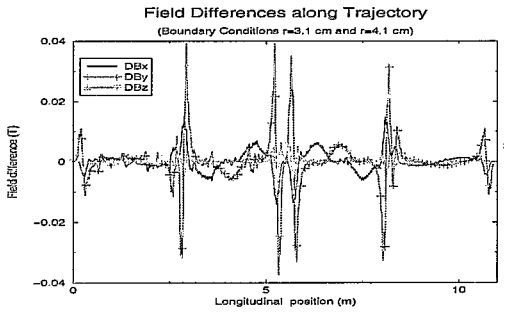

Figure 3: delta B_x ,delta B_y and delta B_z fields evaluated along 100 GeV particle path comparing $\rho = 3.1$ cm to a 4.1 cm

previous predictions, however construction errors lead to an exiting orbit kick of -0.289 mm and -0.489 mm in the x and y direction respectively. In addition the particle picked up a momentum kick of -0.46 mrad and -1.21 mrad in x' and y'.

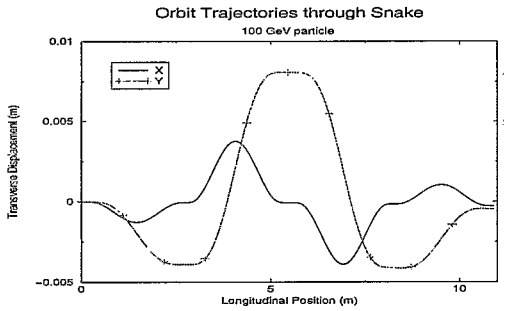

Figure 4: X and Y trajectories through full snake.

A quick evaluation of the orbit paths for particles entering close to the axis and small transverse momentum yielded the following transfer matrix:

$$M = \begin{pmatrix} 0.9964174 & 10.980413 & 0.0014789 & 0.0011432 \\ -0.000656 & 0.9985205 & 0.0002366 & 0.0000774 \\ 0.0001979 & 0.0126185 & 0.9883464 & 10.924713 \\ 0.0002217 & 0.0038101 & -0.002115 & 0.9880669 \end{pmatrix}$$

which yields a $|M| = 1.002$ from this matrix it is clear that the snakes does induce some coupling. The contribution of this coupling to spin resonances has been evaluated [9] showing a strength on the order of coupling caused by the operation of the solenodial field in both PHENIX and STAR detectors. Checking for simplecticity gives:

$$M^T \cdot S \cdot M = \begin{pmatrix} 0 & 1.002 & 0.000017 & -0.0021 \\ -1.002 & 0 & -0.0027 & -0.029 \\ -0.000017 & 0.0027 & 0 & 1 \\ 0.0021 & 0.029 & -1 & 0 \end{pmatrix}$$

Clearly this is inadequate for tracking purposes and more work must still be dones to improve the simplecticity of the snake matrix. As well a more robust technique needs to be employed to calculate the transfer maps up to second order similar to [8].

3 SPIN TRAJECTORY

Considering the behavior of spin through the snake we found our results matched fairly well with previous predictions. With the outer two magnets set at 102 Amps and the inner two at 329 amps the particle achieved a complete spin flip.

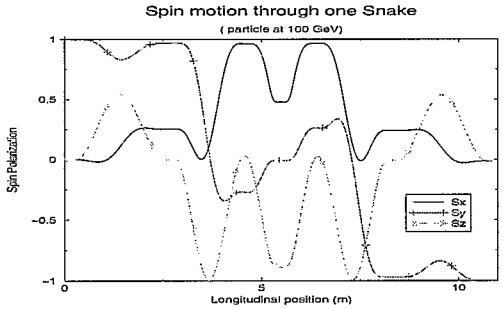

Figure 5: Sx Sy Sz Spin trajectories through full snake. Starting off with Sy=1 polarization

Work needs still to done in evaluating the fields for the rest of the snakes and rotators in RHIC and running orbital and spin tracking under these fields. Work supported under U.S.D.O.E.

4 REFERENCES

[1] TOSCA and OPERA commercial software.

[2] A.U.Luccio, Trends in Collider Spin Physics pp 244 World Scientific (1997)

[3] E.D. Courant, Orbit Matrices for Helical Snakes AGS/RHIC/Spin Note, BNL No. 4 (1996)

[4] E.D. Courant, Hybrid Helical Snakes and Rotators for RHIC, AGS/RHIC/Spin Note, BNL No. 10 (1996)

[5] M.J.Syphers, Closed Orbit Errors from Helical Dipole Magnets, AGS/RHIC/Spin Note, BNL No. 16 (1996)

[6] K.Hatanaka, T.Katayama,T.Tominaka, Maxwellian Field Expansion of Helical Magnet, IEEE 3416 (1998).

[7] W.Fischer, M. Okamura, Parameterization and measurements of Helical Magnetic Fields, IEEE 3341 (1998).

[8] A.U.Luccio, Field Map Generated Matrices for Spin Tracking, RIKEN-AF-NP-235 (1996)

[9] V.Ranjbar,S.Y.Lee,W.W.MacKay,M.Bai,E.Courant, Mapping out the full spin Resonance structure of RHIC, PAC2001 paper to be submitted

Similarly, the maximum value of $\hat{\beta}$ in the interaction region triplet is inversely proportional to the value of β*. By analogy with the equation above, this relationship is conveniently described by introducing the nearly constant "effective triplet distance" $\hat{d}$, which is defined by

$$\hat{d} = (\hat{\beta}\,\beta^*)^{0.5}$$

The effective triplet distance also relates the angular beam size at the IP to the maximum beam size ˆσ, since

$$\hat{\sigma} = \hat{d}\,\sigma'^*$$

The upper limit of this maximum beam size is constrained by the requirement of an aperture at least n≈8 times the rms size of the beam in the triplet quadrupoles. Thus, the angular beam size at the IP must be less than a critical value σ'^*_c which is proportional to the "effective angular aperture" of the triplet, $a/\hat{d}$, through

$$\sigma'^* \le \sigma'^*_c = a/\hat{d}\,n$$

Note that the critical value σ'^*_c is independent of emittance for non-pathological values of β*. The effective angular aperture is the principal figure of merit measuring the potency of IP optics schemes. It is improved by using larger bore quadrupoles (increasing a) or by moving the triplet closer to the IP (decreasing $\hat{d}$).

At RHIC, the Effective triplet distance, $\hat{d}$ is 36 m, the triplet bore radius, a, is 65 mm and this leads to a maximum angular beam size σ'^*_c of 226 μrad, a limit which will be slightly violated if a gold beam with an emittance of ε=40 π μm is stored in a lattice with β*=1 m. With these values, and f_{rev}= 78.3 kHz, we get

$$L=(N_B/120)(\xi/.004)^2(\sigma'^*/226\mu\text{rad})^2 4.6\cdot 10^{28}\ \text{cm}^{-2}\text{s}^{-1}$$

The next natural question to ask is what are the limits on N_B. The image current of the beam which flows in the vacuum chamber walls causes resistive heating. This is not a concern in the sections of beam pipe at room temperature, but has the potential to be a serious problem when the heat is deposited at cryogenic temperatures. A maximum average cryogenic heat load of about 0.5 to 1.0 Watt per meter can be tolerated during continuous running. An analysis [7] lead to the engineering decision to use stainless steel beam pipes without a copper coating. Fig. 1 shows the extension of that analysis to the RHIC upgrades. The linear power load depends strongly on the RMS Gaussian bunch length, and on the number of bunches.

The calculation assumes that all ion bunches have exactly the same charge, and that they are spread uniformly around the circumference. In this case the power spectrum is a series of narrow lines uniformly spaced by $N_B f_{rev}$, under a Gaussian envelope which is the Fourier transform of the bunch shape. The total linear power load is just a sum over all these spectral lines, convoluted with the vacuum chamber resistance at those frequencies – a resistance that is dominated by skin depth effects. As the number of bunches increases, the spacing between spectral lines increases like N_B, but the power in each harmonic increase like N_B^2. Thus when the bunches are longitudinally spaced by very many bunch lengths – for example, when N_B=360 – the linear power load is just proportional to N_B, as is intuitively expected.

Fig. 1 shows that this scaling breaks down when there are 2520 bunches in an ion ring, and the bunch spacing is only 1.52 m, except for very short bunch lengths less than, say, 0.25 m. The suppression of the linear power load which is implied for longer bunch lengths is weakened in more realistic situations – for example, when an abort gap is present and when the bunch populations are not all equal. Nonetheless, it is possible to store as many as 2520 bunches in the ion rings without violating the maximum heat load limit, and without losing much luminosity to the hourglass effect.

Other possible limits, which will not be discussed here, are heating of the Beam Position Monitor signal cables and the electron cloud effect.

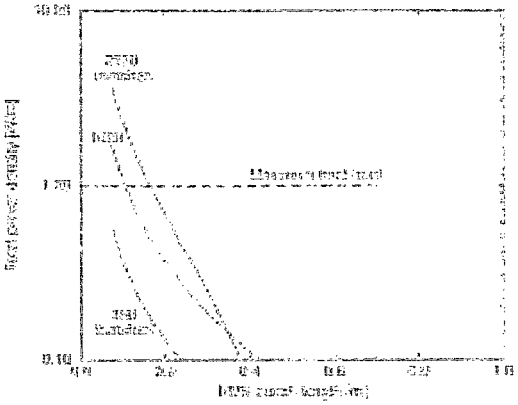

Figure 1. Linear power load deposited at cryogenic temperatures in the stainless steel vacuum chamber, due to beam image currents with 10^9 gold particles per bunch.

5 REFERENCES

[1] I. Ben-Zvi et al., "Electron Cooling for RHIC", Proc. of the Part. Acc. Conf. 2001, Chicago (2001).

[2] J. Allesi et al., "Progress in he Operation of a High Intensity EBIS at BNL", Proc. of the Part. Acc. Conf. 2001, Chicago (2001).

[3] Phillip J. Bryant and Kjell Johnsen, "The Principles of Circular Accelerators and Storage Rings", Cambridge Univ. Press (1993).

[4] Steven D. Holmes, "Tevatron Performance Goals for the Coming Decade", Proc. of the Part. Acc. Conf. 1999, p. 43, New York City (1999).

[5] V. Shiltsev et al., "Compensation of Beam-Beam Effects in the Tevatron Collider with Electron Cooling", Proc. of the Part. Acc. Conf. 1999, p. 3728, New York City (1999).

[6] RHIC Design Manual, BNL, 1993.
http://www.agsrhichome.bnl.gov/NT-share/rhicdm

[7] A.G. Ruggiero, S. Peggs, "Vacuum Pipe Heating in RHIC", RHIC/AP/46, BNL, 1994.